J|A|C|S
ARTICLES
Published on Web 04/30/2004

Local and Global Chirality at Surfaces: Succinic Acid versus Tartaric Acid on Cu(110)

Vincent Humblot, Maria Ortega Lorenzo, Christopher J. Baddeley,† Sam Haq, and Rasmita Raval*

Contribution from the The Surface Science Research Center, Department of Chemistry, University of Liverpool, Liverpool L69 3BX, United Kingdom

Received August 29, 2003; E-mail: raval@liv.ac.uk

Abstract: A detailed comparison of tartaric acid (HOOC−CHOH−CHOH−COOH) and succinic acid (HOOC−CH_2−CH_2−COOH) molecules on a Cu(110) surface is presented with a view to elucidate how the two-dimensional chirality exhibited by such robust, chemisorbed systems is affected when both OH groups of the former molecule are replaced with H groups, a stereochemical change that leaves the metal-bonding functionalities of the molecule untouched but destroys both chiral centers. It is found that this change does not significantly affect the thermodynamically preferred chemical forms that are adopted, namely the doubly deprotonated bicarboxylate at low coverages ($\theta \leq {}^1/_6$ ML) and the singly deprotonated monocarboxylate at higher coverage. However, the kinetics of phase formation are significantly affected so that the conditions required for self-assembling pertinent two-dimensional chiral phases alter substantially. For both molecules, two-dimensional assembly is found to depend strongly on the nature of the local adsorption motif created, with each motif essentially acting as a "synthon" for the supramolecular assembly. In this respect, it seems that molecule−metal bonding interactions define the general self-assembly structure. The presence/absence of the OH groups, instead, cause a subtler, second-order effect on the finer details of the self-assembled structure. Finally, the creation of chirality in the achiral succinate system is shown to arise from adsorption-induced asymmetrization, inducing point chirality via molecular distortion and/or metal reconstruction of the local adsorption unit. This chiral adsorption unit is then responsible for creating chiral supramolecular through-space and through-metal interactions that propagate a chiral organization. However, the achirality of the succinate ensures that nucleation points of either chirality are equally created, producing a racemic conglomerate of coexisting mirror domains. It is in this aspect that the uniquely aligned OH groups of the rigid bitartrate system wield the greatest effect, by favoring one distortion/reconstruction for the (*R*,*R*)-bitartrate and its mirror image distortion/reconstruction for the (*S*,*S*)-enantiomer, creating surfaces that are globally chiral on the macroscopic scale. So overall, the OH groups do not dictate the general nature of the assembly but are critical as chiral propagators, breaking the degeneracy and thus promoting asymmetry to chirality.

1. Introduction

Although chiral surfaces offer intriguing possibilities in a range of technological fields such as nonlinear optical materials, heterogeneous enantioselective catalysis and sensor devices, it is only recently that the manifestation of chirality in two dimensions has been captured with the advent of sophisticated surface science techniques.[1−23] A particularly successful way of endowing nonchiral metal surfaces with chirality is via the adsorption of complex organic molecules. The presence of the organic functionality serves to inject the ultimate selectivity

† Present address: School of Chemistry, North Haugh, University of St. Andrews, St. Andrews KY16 9ST, United Kingdom.

(1) Barlow, S. M.; Raval, R. *Surf. Sci. Rep.* **2003**, *50*, 201.
(2) Raval, R. *Curr. Opin. Solid State Mater. Sci.* **2003**, *7*, 67.
(3) Ortega Lorenzo, M.; Baddeley, C. J.; Muryn, C.; Raval, R. *Nature* **2000**, *404*, 376.
(4) Ortega Lorenzo, M.; Haq, S.; Bertrams, T.; Murray, P.; Raval, R.; Baddeley, C. J. *J. Phys. Chem. B* **1999**, *103(48)*, 10661.
(5) Humblot, V.; Haq, S.; Muryn, C.; Hofer, W.; Raval, R. *J. Am. Chem. Soc.* **2002**, *124*, 503.
(6) Jones, T. E.; Baddeley, C. J. *Surf. Sci.* **2002**, *513*, 453.
(7) Jones, T. E.; Baddeley, C. J. *Surf. Sci.* **2002**, *519*, 237.
(8) Ernst, K. H.; Kuster, Y.; Fasel, R.; Muller, M.; Ellerbeck, U. *Chirality* **2001**, *13*, 675.
(9) Ortega Lorenzo, M.; Humblot, V.; Murray, P.; Baddeley, C. J.; Haq, S.; Raval, R. *J. Catal.* **2002**, *205*, 123.
(10) Raval, R. *CATTECH* **2001**, *5*, 12.
(11) Zhao, X. *J. Am. Chem. Soc.* **2000**, *122*, 12584.
(12) Kühnle, A.; Linderoth, T. R.; Hammer, B.; Besenbacher, F. *Nature* **2002**, *415*, 891.
(13) De Feyter, S.; Gesquiere, A.; Wurst, K.; Amabilino, D. B.; Veciana, J.; De Schryver, F. C. *Angew. Chem., Int. Ed.* **2001**, *40*, 3217.
(14) Barth, J. V.; Wechesser, J.; Trimarchi, G.; Vladimirova, M.; De Vita, A.; Cai, C.; Brune, H.; Günter, P.; Kern, K. *J. Am. Chem. Soc.* **2002**, *124*, 7991.
(15) Lopinski, G. P.; Moffat, D. J.; Wayner, D. D.; Wolkow, R. A. *Nature* **1998**, *392*, 909.
(16) Barlow, S. M.; Kitching, K. J.; Haq, S.; Richardson, N. V. *Surf. Sci.* **1998**, *401*, 322.
(17) Weckesser, J.; Barth, J. V.; Cai, C.; Muller, B.; Kern, K. *Surf. Sci.* **1999**, *431*, 168.
(18) Schunack, M.; Petersen, L.; Kühlne, A.; Laegsgaard, E.; Stensgaard, I.; Johannsen, I.; Besenbacher, F. *Phys. Rev. Lett.* **2001**, *86*, 456.
(19) Viswanathan, R.; Zasadzinski, J. A.; Schwartz, D. K. *Nature* **1994**, *368*, 440.
(20) Böhringer, M.; Morgenstern, K.; Schneider, W.-D.; Berndt, R. *Angew. Chem., Int. Ed.* **1999**, *38*, 821.
(21) McFadden, C. F.; Cremer, P. S.; Gellman, A. J. *Langmuir* **1996**, *12*, 2483.
(22) Attard, G. A. *J. Phys. Chem. B* **2001**, *105*, 3158.

10.1021/ja0382056 CCC: $27.50

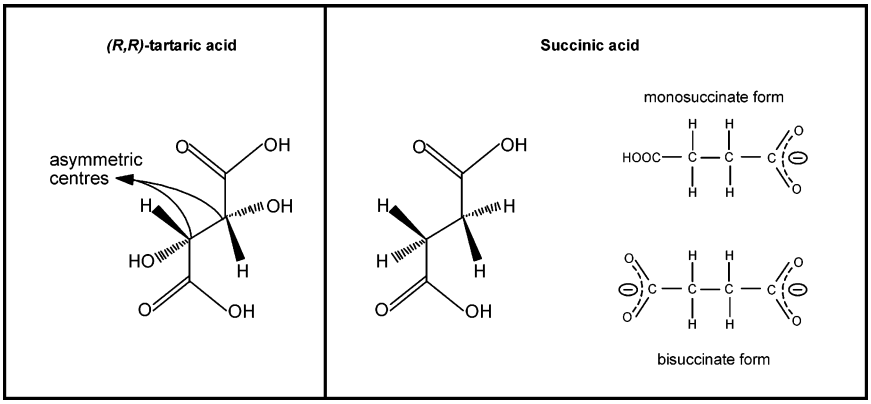

Figure 1. Diagram showing the molecules (*R*,*R*)-tartaric acid and succinic acid and the different chemical forms that can be adopted by the latter upon adsorption.

attribute of chirality onto the already reactive metal catalyst. There is a manifold of chiral expressions that can be realized via this approach from the creation of local chiral motifs to the supramolecular assembly of chiral organizations, and these have been reviewed elsewhere.[1,2] Interestingly, it is found that chiral exhibition is not simply limited to systems in which chiral molecules are adsorbed at achiral surfaces[2−12] but rather can also be displayed in systems where no initial chirality is present, i.e., from the adsorption of achiral molecules at achiral surfaces.[13−20] Much of the work published on aspects of two-dimensional chirality deals with physisorbed or weakly adsorbed systems,[13,19,20] and less is understood about strongly chemisorbed systems, especially the subtle influences of stereochemical alterations on both the local and the organizational characteristics. For such systems, where a strong molecule−metal interaction exists, a very rich adsorption phase space can often be occupied where the nature of the adsorbate can change significantly with coverage and temperature. Thus, a deeper understanding of the factors that affect two-dimensional chirality requires a range of spectroscopic techniques that not only probe the nature of extended supramolecular assemblies but also are able to tie that information with the detailed nature of the local adsorption unit that essentially acts as a "synthon" for the supramolecular structure. A case in point is the behavior of the chiral molecule, (*R*,*R*)-tartaric acid, on the achiral Cu(110) surface[1−4,9] where chiral expression encompasses both the creation of a variety of local chiral motifs and a range of supramolecular chiral assemblies, with the nature of the former intimately controlling the nature of the latter. In this work, we investigate how the expression of two-dimensional chirality in this strongly chemisorbed system is affected if the two chiral centers of (*R*,*R*)-tartaric acid are removed. Thus, we report on the adsorption of succinic acid on Cu(110) and compare the results obtained with those found for (*R*,*R*)-tartaric acid. Succinic acid is a very similar molecule to tartaric acid, with the only difference being that the two hydroxyl groups present in tartaric acid are replaced by hydrogen atoms leading to a consequent loss of both chiral centers, Figure 1. To compare and contrast these two systems at both the local adsorption motif level and at the extended self-organization level, we have applied the surface science techniques of reflection absorption infrared spectroscopy (RAIRS) to provide detailed chemical and orientational information on the adsorbate, temperature programmed desorption (TPD) to yield information on the adsorbate−metal bonding, and low energy electron diffraction (LEED) and scanning tunneling microscopy (STM) to investigate the self-organizational behavior of the systems.

2. Experimental Section

Two ultrahigh vacuum (UHV) chambers were used in this study. The first chamber contained facilities for FT-RAIRS, TPD, LEED, and sample cleaning. This chamber was interfaced with a Mattson 6020 FT-IR spectrometer equipped with a liquid nitrogen cooled HgCdTe detector with a spectral range of 650−4000 cm^{-1}. RAIRS spectra were recorded throughout a continuous dosing regime as sample single beam infrared spectra and ratioed against a reference background single beam of the clean Cu(110) crystal. All spectra were obtained at 4 cm^{-1} resolution with coaddition of 256 scans. TPD spectra were collected between 273 and 630 K by heating the Cu(110) crystal while measuring the change in partial pressure for masses 2, 26, 28, and 44 as a function of sample temperature. Heating rates of ∼2 K s^{-1} were used in TPD experiments. A CCD video camera interfaced to a computer was used for the digitization of the LEED patterns.

The second chamber was an Omicron Vakuumphysik variable temperature VT-STM chamber with facilities for STM, LEED, AES, and sample cleaning. All STM experiments were carried out with the sample at room temperature. The images were acquired in constant current mode.

In each chamber, the Cu(110) crystal was cleaned by cycles of Ar^+ ion sputtering, flashing, and annealing to 800 K. The surface ordering and cleanliness were monitored by LEED and AES. Succinic acid (99%)and (*R*,*R*)-tartaric acid (99%) were obtained from Sigma Aldrich and used without further purification. The adsorbate sample was contained in a small resistively heated glass tube, separated from the main vacuum chamber by a gate valve and differentially pumped by a turbo molecular pump. Before sublimation, the sample was outgassed at ∼330−340 K. The sample was then heated to ∼370 K and exposed to the copper crystal. During sublimation the main chamber pressure was typically 2×10^{-9} mbar. The copper crystals were provided by Surface Preparation Laboratory (The Netherlands) with a purity of 99.99% (4N), and alignment accuracies of 0.5 ° and 0.1° for the RAIRS and the STM experiments, respectively.

Each overlayer unit cell in this paper is described by the matrix:

$$\begin{pmatrix} a_o \\ b_o \end{pmatrix} = \begin{pmatrix} m_{11} & m_{12} \\ m_{21} & m_{22} \end{pmatrix} \begin{pmatrix} a_s \\ b_s \end{pmatrix}$$

where $\mathbf{a_o}$, $\mathbf{b_o}$ are the overlayer unit vectors; $\mathbf{a_s}$, $\mathbf{b_s}$ are the substrate unit

(23) Scholl, D. S.; Asthagiri, A.; Power, T. D. *J. Phys. Chem. B* **2001**, *105*, 4771.

vectors; and $|\mathbf{a}_s| < |\mathbf{b}_s|$ with the vectors all defined by a right-handed axis system. Further details on the conventions used can be found in ref 1.

3. Results and Discussion

The chiral influence of (*R*,*R*)-tartaric acid on Cu(110) can be discerned at two levels: first, at the local level where adsorption events conserve the chiral centers and, thus, give rise to point chirality and, second, at the organizational level where self-assembled structures form that are chiral in arrangement and, thus, destroy the mirror symmetry elements possessed by the underlying surface.[1−4,9] Various phases are observed for (*R*,*R*)-tartaric acid on Cu(110),[4] and in the comparison here, we concentrate simply on the low coverage phases, namely the c(4 × 2) phase created at room temperature (300 K) and the (1 2, −9 0) phase created at a higher temperature (400 K). RAIRS data have shown that the former phase consists of the monotartrate unit that bonds to the surface via its single carboxylate functionality, while the latter phase consists of the doubly deprotonated bitartrate species bonded with both carboxylate groups to the metal surface with the C_2-C_3 bond parallel to the surface. Density functional calculations[24] confirm this general adsorption configuration for the bitartrate and, additionally, show that the adsorption site is across the long-bridge site on the Cu(110) surface with each of the four carboxylate oxygens placed on top of a metal atom. Although the bitartrate unit is thermodynamically preferred at low coverages, the monotartrate unit forms upon initial adsorption at room temperature due to kinetic factors, and only upon heating to 400 K, is the bitartrate phase created. An activation barrier of ∼73 kJ mol^{-1} is associated with this transformation.[9]

To compare and contrast the behavior of succinic acid, both the local and the organizational aspects were probed in the 300−400 K temperature range under conditions where the low coverage monotartrate and bitartrate phases of tartaric acid are created. Like tartaric acid, succinic acid is capable of existing in at least three different forms: the neutral bi-acid form, the monosuccinate form where one of the carboxylic groups has deprotonated, and the bisuccinate form in which both acid groups have deprotonated, Figure 1. Given that the local adsorption unit essentially acts as a "synthon" for the supramolecular structure, we first utilized the RAIRS technique to determine the nature of the adsorbed species, as discussed below.

3.1. Nature of the Local Adsorption Unit: The Monosuccinate and Bisuccinate Forms. Figure 2 shows the RAIR spectra for increasing coverages of succinic acid on a Cu(110) surface held at 300 K. At low coverages, Figure 2a, the only bands of significant intensity are at around 1400 cm^{-1}. In particular, no band at 1700 cm^{-1} due to the normally strong $\nu_{C=O}$ stretching vibration is present, indicating that no carboxylic acid groups are present in the adsorbed species. The 1425, 1408 cm^{-1} doublet also shows striking similarity to that displayed by the bitartrate form of tartaric acid[4,9] where a doublet at 1430 and 1410 cm^{-1} was assigned, on the basis of model spectra for dipotassium tartrate[25] and Rochelle salt,[26] to the coupled vibrations of the identical COO^- oscillators on each molecule.

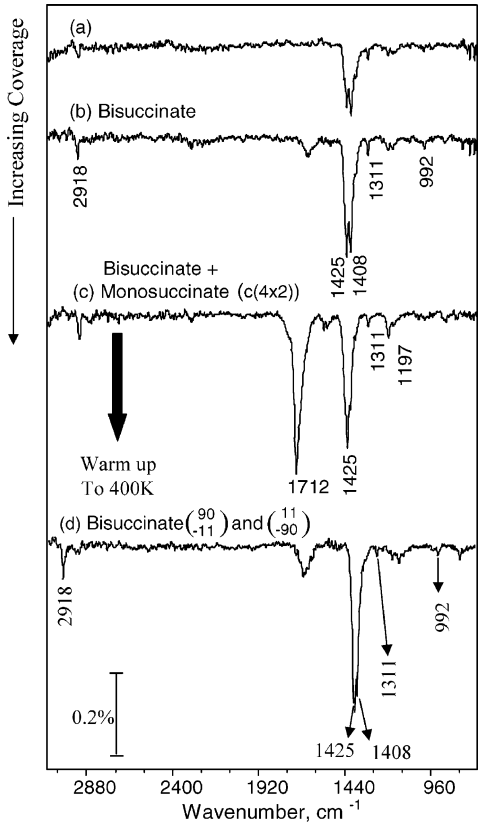

Figure 2. RAIR spectra observed as a function of increasing coverage of succinic acid adsorbed on Cu(110) at 300 K and when the temperature is increased up to 400 K. The IR bands give direct information on the chemical nature and general orientation of the adsorbed species.

We, therefore, assign these low coverage spectra to a doubly deprotonated bisuccinate species at the surface with the doublet bands assigned to the $\nu^{sym}_{OCO^-}$ symmetric carboxylate stretch. The hydrogens created by the deprotonation process undergo recombinative desorption, a process that has been well documented for Cu surfaces at room temperature.[27−29]

An important clue to the adsorption geometry of the bisuccinate species is the absence of the corresponding $\nu^{asym}_{OCO^-}$ asymmetric carboxylate vibration at ∼1600 cm^{-1}. Utilizing the RAIRS dipole selection rule, this absence can be attributed to a configuration in which each COO^- unit has bidentate coordination with the two oxygen atoms held almost equidistant from the surface, thus significantly attenuating the asymmetric stretch. This functional orientation, when applied to both carboxylate groups of the molecule, naturally forces the molecular C_2-C_3 axis parallel to the surface. Such an adsorption geometry again mimics the behavior of the bitartrate system. It is rather more difficult to extend such analysis further to determine the orientations of the CH_2 groups, since the vibrations of these functional groups possess intrinsically weaker intensities and are, therefore, difficult to record reliably. Nevertheless, the presence of the symmetric $\nu^{sym}_{CH_2}$ stretch can be unambiguously identified at 2918 cm^{-1}, while the asymmetric $\nu^{asym}_{CH_2}$ stretch, expected at 2980 cm^{-1}, is not observed, suggesting that the methylene group is oriented largely symmetrically

(24) Barbosa, L. A. M. M.; Sautet, P. *J. Am. Chem. Soc.* **2001**, *123*, 6639.
(25) Srivastava, G. P.; Mohan, S.; Jain, Y. S. *J. Raman Spectrosc.* **1982**, *13*, 25.
(26) Bhattacharjee, R.; Jain, Y. S.; Raghubanshi, G.; Bist, H. D. *J. Raman Spectrosc.* **1988**, *19*, 51.
(27) Tabatabaei, J.; Sakakini, B. H.; Watson, M. J.; Waugh, K. C. *Catal. Lett.* **1999**, *59*, 143.
(28) Tabatabaei, J.; Sakakini, B. H.; Watson, M. J.; Waugh, K. C. *Catal. Lett.* **1999**, *59*, 151.
(29) Genger, T.; Hinrichsen, O.; Muhler, M. *Catal. Lett.* **1999**, *59*, 137.

Table 1. Characteristic Vibrational Bands (cm^{-1}) and Assignments for Solid Succinic Acid[30] and Solid Tartaric Acid,[31] the Monotartrate Phase on Cu(110),[4] the Monosuccinate Phase on Cu(110), the (*R*,*R*)-Bitartrate Phase on Cu(110),[4] and the Bisuccinate Phase on Cu(110)[a]

Tartaric acid powder [31] (cm^{-1}, assignment).		Succinic acid crystal [30] (cm^{-1}, assignment).		(*R*,*R*)-tartaric acid monotartrate [4] (cm^{-1}, assignment).		Succinic acid monosuccinate (cm^{-1}, assignment).		(*R*,*R*)-tartaric acid bitartrate [4] (cm^{-1}, assignment).		Succinic acid bisuccinate (cm^{-1}, assignment).	
3388 br,s 3315 br,s	ν_{OH}^{alc}										
3193 br, s 3083 br, s	ν_{OH}^{acid}	2990 br,s	ν_{OH}^{acid}								
2972 br 2939 br	ν_{CH}	2980 br, s 2930 br, s	$\nu_{CH_2}^{asym}$ $\nu_{CH_2}^{sym}$			2918 w	$\nu_{CH_2}^{sym}$			2918 vw	$\nu_{CH_2}^{sym}$
1741 br,vs	$\nu_{C=O}$	1729 s 1690 s	$\nu_{C=O}$	1711 s	$\nu_{C=O}$	1712 s	$\nu_{C=O}$				
1453 br, s	ν_{C-O}^{acid}	1418 m	$\delta_{CH_2}^{scissor}$ $\nu_{C-O}^{acid}+\delta_{OH}^{acid}$	1437 s	ν_{OCO}^{sym}	1425 s	ν_{OCO}^{sym} $\delta_{CH_2}^{scissor}$ $\nu_{C-O}^{acid}+\delta_{OH}^{acid}$	1430 s 1410 s	ν_{OCO}^{sym}	1425 s 1408 s	ν_{OCO}^{sym} $\delta_{CH_2}^{scissor}$
1375 s	δ_{OH}^{alc}			1398 w 1378 w	δ_{OH}^{alc}			1375 so	δ_{OH}^{alc}		
1318 w 1255 m 1220 m	δ_{OH}^{acid} $+\ \delta_{CH}$	1308 m	$\nu_{C-O}^{acid}+\delta_{OH}$ γ_{CH_2}	1338 w 1300 w 1234 m 1197 w	δ_{OH}^{acid} $+\ \delta_{CH}$	1311 w	$\nu_{C-O}^{acid}+\delta_{OH}$ γ_{CH_2}	1338 s 1200 w	δ_{CH}	1311 vw	γ_{CH_2}
		1203 m	$\delta_{CH_2}^{wagging}$			1197 w	$\delta_{CH_2}^{wagging}$ $\delta_{CH_2}^{twisting}$			1197 w	$\delta_{CH_2}^{wagging}$ $\delta_{CH_2}^{twisting}$
1190 m 1134 m 1087 m	ν_{C-O}^{alc}	1175 vw	$\delta_{CH_2}^{twisting}$	1101 m	ν_{C-O}^{alc}			1113 s	ν_{C-O}^{alc}		
992 vw	ν_{C-C}							999 vw	ν_{C-C}	992 vw	ν_{C-C}

[a] s, m, w, v, br, and so indicate strong, medium, weak, very, broad, and shoulder, respectively.

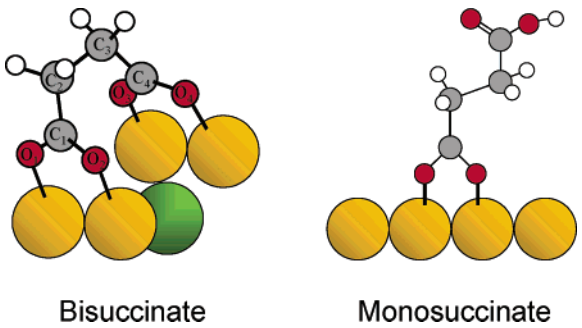

Figure 3. Schematic representation of the succinic acid molecule adsorbed in its bisuccinate and monosuccinate forms on the Cu(110) surface.

with respect to the surface normal. Detailed vibrational assignments of the bisuccinate species are given in Table 1, but it should be appreciated that bands in the range 1300−900 cm^{-1} are very low in intensity and, therefore, difficult to assign unambiguously. However, overall, the RAIRS spectra are consistent with the adsorption geometry shown in Figure 3, which also agrees well with density functional theory calculations of the bisuccinate species on Cu(110).[24]

As coverage is increased, Figure 2 (b) and (c), a strong band at 1712 cm^{-1} appears due to a $\nu_{C=O}$ stretching vibration, indicating the presence of a second species at the surface in which the COOH acid group is retained. The similarity of this band with that found in the monotartrate form of tartaric acid strongly suggests that the additional molecules are accommodated on the surface in the monosuccinate form. The frequency of the $\nu_{C=O}$ vibration indicates the presence of considerable H-bonding interactions, probably involving COOH/COOH intermolecular interactions of the type seen for crystalline succinic acid.[30] The second band that can be associated with the monosuccinate species is the 1197 cm^{-1} band, whose growth behavior follows that of the 1712 cm^{-1} band. On the basis of the IR spectra of crystalline succinic acid,[30] this band may be assigned to either the $\delta_{CH_2}^{wagging}$ or the $\delta_{CH_2}^{twisting}$ deformation, Table 1. The monosuccinate species will, of course, also possess vibrations for the deprotonated carboxylate group that bonds to the surface. However, when the bisuccinate and monosuccinate coexist, it is difficult to disentangle the contributions made by each to the symmetric $\nu_{OCO^-}^{sym}$ vibration region. Here, we note that even for the monosuccinate phase, no asymmetric $\nu_{OCO^-}^{asym}$ stretch is observed, again placing the carboxylate group in a symmetrical stance at the surface, Figure 3. Finally, the monosuccinate phase should also possess vibrations from the C−OH group of the acid functionality. However, the only expected bands arise from coupled δ_{OH}^{acid} and $\nu_{C=O}$vibrations at ∼1418 and 1308 cm^{-1} [30] and, thus, overlap with the vibrations of the coexisting bisuccinate species, Table 1.

When the coexistence phase, represented by Figure 2c, is annealed up to ∼400 K, Figure 2d, a monosuccinate → bisuccinate interconversion is observed, with loss of intensity of the monosuccinate bands and increase in intensity of the bisuccinate bands. This behavior indicates that the monosuccinate form remains inherently unstable with respect to the bisuccinate form throughout this low coverage regime and is only created at 300 K due to kinetic barriers, probably due to lack of suitable adjacent sites which can accommodate bonding of both carboxylate functionalities. Upon annealing, the adlayer is able to relax into the thermodynamically favorable bisuccinate conformation. This preference continues until the entire surface

(30) Suzuki, M.; Shimanouchi, T. *J. Mol. Spectrosc.* **1968**, *28*, 394.
(31) Bhattacharjee, R.; Jain, Y. S.; Bist, H. D. *J. Raman Spectrosc.* **1989**, *20*, 91.

is covered in the bisuccinate phase. Finally, when coverage is pushed beyond this threshold point, the bisuccinate is now destabilized with respect to the monosuccinate and, in an identical manner to that reported for the tartaric acid system,[4,9] further adsorption is accompanied by a reverse bisuccinate → monosuccinate transformation via the following suggested route:

$$\underset{\text{adsorbed bisuccinate}}{OOCCH_2CH_2COO\ (a)} + \underset{\text{incoming bi-acid}}{HOOCCH_2CH_2COOH} \rightarrow \underset{\text{adsorbed monosuccinate}}{2OOCCH_2CH_2COOH\ (a)}$$

The vibrational analysis presented above reveals that, overall, the local chemistry of succinic acid at Cu(110) tracks that of tartaric acid and the presence of the OH groups does not make a big difference.

However, one interesting point of difference is the kinetics of phase formation in the low coverage regime where the bicarboxylate is thermodynamically favored for both systems. The bisuccinate phase is created readily upon initial adsorption at 300 K, and only with increasing coverage does a kinetic barrier to its formation emerge, allowing the monosuccinate to be formed instead. In contrast, adsorption of tartaric acid at 300 K never leads to the formation of the bitartrate species, and instead, islands of monotartrate molecules are always formed upon adsorption at 300 K.[4,9] Conversion to the thermodynamically preferred bitartrate species then only occurs when temperature is raised to 400 K. We attribute this general behavior to an increased propensity for intermolecular interactions in the tartaric acid system due to additional COOH/OH hydrogen bonding interactions between the acid groups and hydroxyl groups of adjacent monotartrate molecules.[4] This encourages the formation of high density islands, which locally reach the threshold coverage that favors the monotartrate species. Under the flux conditions used in our experiments, the rate of island growth exceeds the rate of the second deprotonation to form the bitartrate species, and so the monotartrate species is formed first.

In contrast, the lack of alcohol groups in succinic acid reduces the propensity for island formation sufficiently so that, under similar flux conditions, the balance is altered and the second deprotonation event is favored to yield the thermodynamically preferred bisuccinate species. In terms of two-dimensional chirality, this means that the conditions required for the creation of a pertinent chiral surface may alter substantially with small changes of molecular structure. Figure 4 illustrates this with a schematic adsorption phase diagram comparing the behavior of both succinic and tartaric acids in the temperature range 300 and 400 K. The different LEED structures found for each characteristic bonding of the molecules are indicated and will be the focus of the next section.

3.2. Organizational Behavior. To compare the behavior of tartaric acid with succinic acid, information on the self-organization of the monosuccinate and bisuccinate phases was probed by LEED and STM studies. Figure 5b shows the LEED patterns obtained after adsorption of succinic acid on a clean Cu(110) surface at 300 K under conditions in which RAIRS data show both the monosuccinate and bisuccinate forms are present. Three distinct structures are observed in the LEED pattern of Figure 5: a c(4 × 2) or (2 1, −4 0) structure associated with the monosuccinate form and two distinct

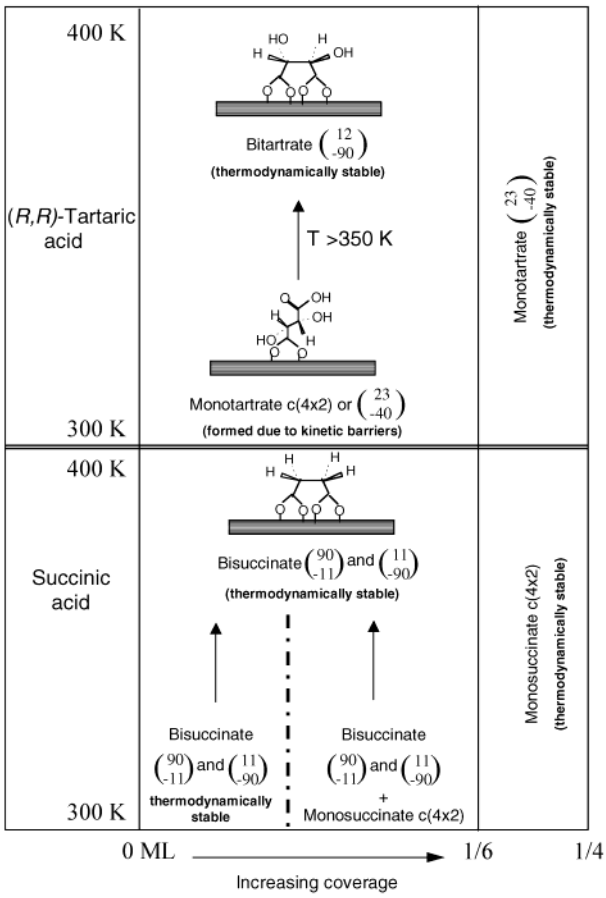

Figure 4. Schematic adsorption phase diagram showing the molecular nature and two-dimensional order adopted by tartaric acid and succinic acid molecules on a Cu(110) surface as a function of coverage, temperature, and time.

(9 0, −1 1) and (1 1, −9 0) structures associated with the bisuccinate form. Schematics of the real space unit cells represented by these LEED structures are shown in Figure 5 (b). For the bisuccinate a large unit cell exists with dimensions 23.04 Å × 4.43 Å with $\alpha = 35.3°$ for the (1 1, −9 0) structure and $\alpha = -35.3°$ for the (9 0, −1 1) structure. To gain more information on the detailed molecular occupation of these unit cells, STM data of the coexistence structure were collected. A large area scan, Figure 5a, shows that domains associated with the monosuccinate and bisuccinate phases can be readily discerned; each is discussed in more detail below.

(i) Monosuccinate Phase. Dealing first with the monosuccinate phase, STM images, Figure 6a, show that the organizational structure imaged is essentially a c(8 × 2), with each STM feature occupying a large area of 6.5 Å × 7.6 Å ± 0.2 Å. Given the RAIRS and LEED information, we propose that the STM features correspond to dimers of monosuccinate adsorbates, organized as shown in Figure 6b. For such a structure, the LEED pattern is determined by the c(4 × 2) arrangement of individual adsorbates while the STM only images the dimers that are presumably held together by COOH−COOH interactions of the type found in succinic acid crystals.[30] The c(4 × 2) arrangement corresponds to a local coverage of 0.25 ML and is identical to that occupied by the monotartrate phase.[4] It would, therefore, seem that the loss of the chiral centers does not materially affect either the density or the organizational packing of this phase. It

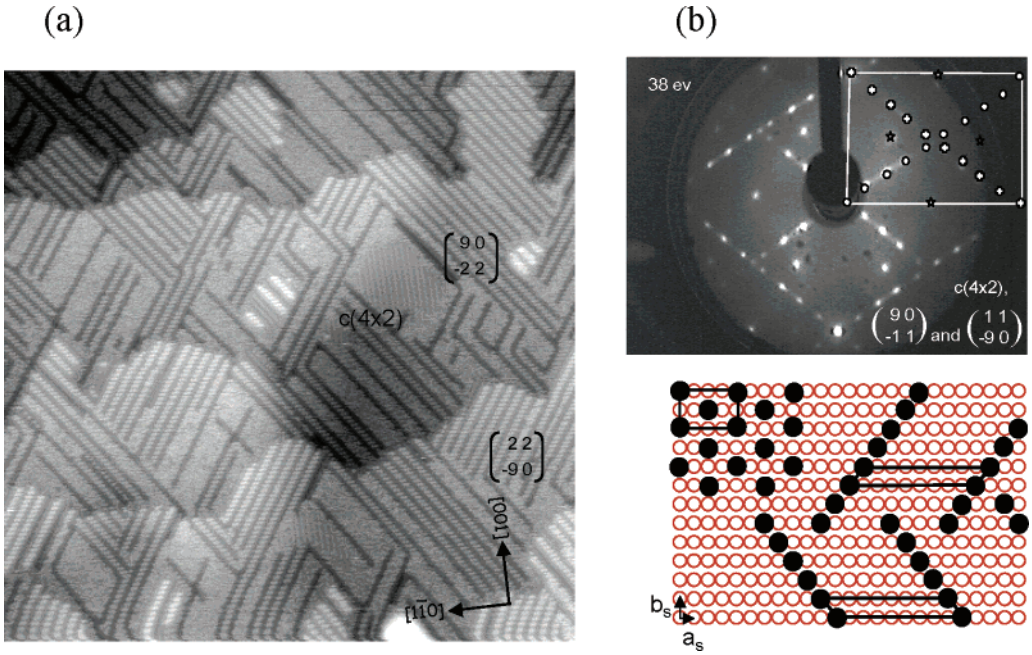

Figure 5. Adsorption of succinic acid on Cu(110) at 300 K gives rise to a number of different adsorption phases as identified by STM and LEED data: (a) STM image showing the coexistence of three phases: the (2 2, −9 0) and (9 0, −2 2) bisuccinate phases and the c(4 × 2) monosuccinate phase. 1000 Å × 1000 Å [$V = -0.23$ V; $I = 0.98$ nA]. (b) LEED pattern observed when succinic acid is adsorbed on Cu(110) at 300 K showing a mixture of c(4 × 2), (9 0,−1 1), and (1 1, −9 0) structures. Schematics of the real space unit cells represented by these LEED structures are shown below.

also does not influence the chirality of the organization which remains as the achiral c(4 × 2) for both the chiral monotartrate[4] and the achiral monosuccinate, Figure 6. Therefore, it would seem that the primary influence on packing and positional organization is determined by the general nature of the adsorption motif and its molecule−metal interactions, in this case, the monocarboxylate−Cu interaction, which is identical for the monosuccinate and the monotartrate. The alterations at the chiral centers cause a lesser, second-order effect, namely in the detail of the supramolecular H-bonding, since the loss of the OH "tail" groups restricts intermolecular interactions of the monosuccinate to cyclic dimers with "head-to-head" COOH−COOH interactions of the type found in succinic acid crystals,[30] rather than the "head to tail" COOH−OH interactions reported for the monotartrate phase.[4]

(ii) Bisuccinate Phase. Turning to the bisuccinate phase, it is clear that it produces two domains at the surface. From the STM images, Figure 7a, detailed structural models on the organization of adsorbates in the two domains can be built, Figure 8a, and it can be seen that each domain consists of rows of three bisuccinate molecules that assemble into long chains at the surface. Crucially, these chains lie along nonsymmetry directions, thus annihilating both reflection planes of the underlying Cu(110) and creating a system where chirality is present at the organizational (space group) level. The imaged (2 2, 9 0) and (9 0, −2 2) molecular unit cells have dimensions 23.04 Å × 8.86 Å with $\alpha = \pm 35.3°$ with a coverage of $^1/_6$ ML, and their structure is remarkably similar to that adopted by the (1 2, −9 0) (*R*,*R*)-bitartrate and (9 0, −1 2) (*S*,*S*)-bitartrate phases (Figure 7b) which also have large repeat unit cells of 23.04 Å × 7.68 Å with $\alpha = \pm 19.47°$, a coverage of $^1/_6$ ML and also display chains of "trimer" molecules that lie along nonsymmetry directions, thus endowing the system with a similar organizational chirality. So again, it appears that the general nature of the bicarboxylate adsorption motif with its

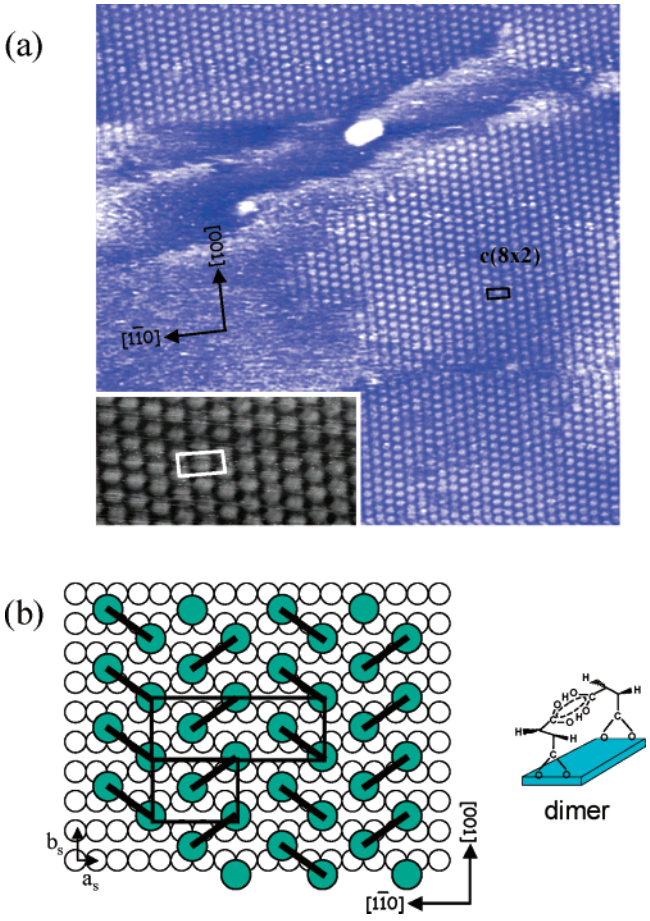

Figure 6. Details of the monosuccinate phase created on Cu(110). (a) STM images ((main) 500 Å × 500 Å and (insert) 60 Å × 120 Å) [$V = -1.39$ V; $I_t = 0.14$ nA] showing the monosuccinate c(8 × 2) phase of succinic acid adsorbed on Cu(110). Structural model showing the c(8 × 2) phase arising as a possible array of dimer motifs.

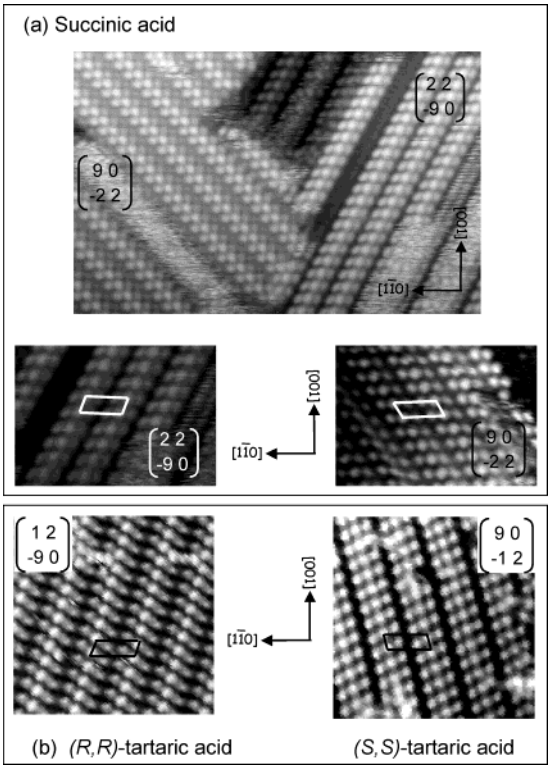

Figure 7. Comparison of the bicarboxylate phases created by the achiral bisuccinate and the chiral bitartrate on Cu(110). (a) Depiction of the bisuccinate phase. STM images (260 Å × 170 Å) [$V = -0.21$ V; $I = 0.15$ nA] showing the coexistence of the (2 2, −9 0) and (9 0, −2 2) domains; each individual domain is also presented in detailed STM images (100 Å × 70 Å) [$V = 0.23$ V; $I = 0.19$ nA]. (b) Depiction of the (1 2, −9 0) and (9 0, −1 2) bitartrate phases formed after the adsorption of (*R*,*R*)-tartaric acid and (*S*,*S*)-tartaric acid, respectively, on Cu(110). STM images (108 Å × 108 Å) [$V = -1.7$ V; $I = 1.18$ nA] showing the (*R*,*R*)-tartaric acid (1 2, −9 0) phase and (108 Å × 108 Å) [$V = -2.73$ V; $I = 1.02$ nA] showing the (*S*,*S*)-tartaric acid (9 0, −1 2) phase.

two COO−Cu bonding interactions is the primary factor determining the overall nature, ordering, density, and chirality of the superstructure adopted, regardless of whether the adsorbed molecule is chiral (tartrate) or achiral (succinate). The comparison between the bisuccinate and bitartrate phases brings new insights into the role of the OH groups in determining the supramolecular assembly. In the first reports of this system,[3] it was assumed that intermolecular hydrogen bonding between neighboring bitartrate molecules governed the nature of the superstructure, forcing growth along nonsymmetry directions. Subsequent DFT calculations[24] showed that the neighboring molecules in the bitartrate structure are too far apart for intermolecular hydrogen bonding interactions to occur and only intramolecular H-bonds were present. These calculations suggested that supramolecular assembly was instead governed via through-space lateral interactions and/or through-metal lateral interactions. What our data shows is that H-bonding interactions of any kind are not the driving force for the chiral assembly, since the bisuccinate is as successful as the bitartrate in creating chiral assembly. Equally, the through-space lateral interactions and/or through-metal lateral interactions must be dominated by the metal−molecule interactions so that both systems produce a similar trimer chain structure. So overall, the presence/absence of the OH groups at the chiral centers does not affect the general type of supramolecular assembly. Instead, their influence is exerted more subtly within the finer detail of the self-assembly.

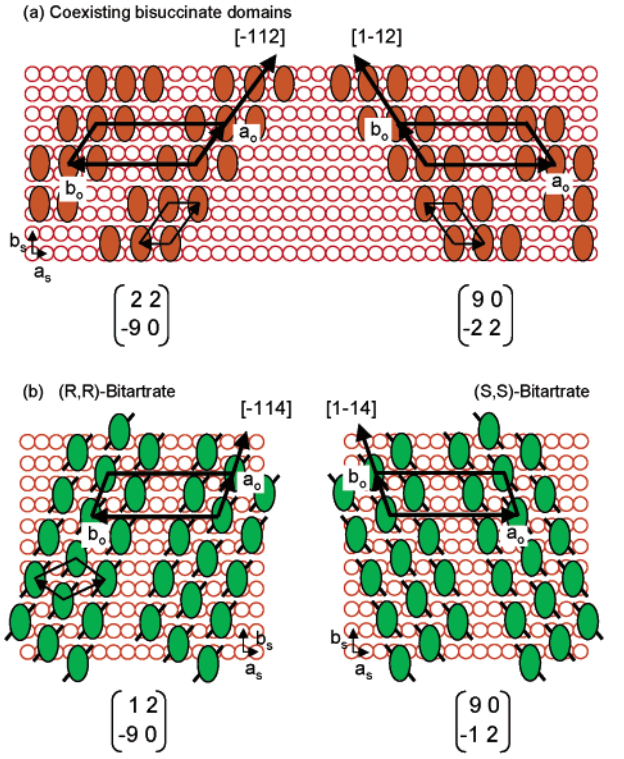

Figure 8. Adsorption models of the bisuccinate and the bitartrate phases on Cu(110). (a) Structural models for the two coexisting chiral domains imaged by STM for bisuccinate on Cu(110). The (2 2, −9 0) and (9 0, −2 2) unit cells of the overall structure are shown as are the (2 2, −2 0) and (2 0, −2 2) unit cells representing the packing within each chain. (b) Structural models of the bitartrate phases of the two tartaric acid enantiomers on Cu(110): (*S*,*S*)-bitartrate (9 0, −1 2) and (*R*,*R*)-bitartrate (1 2, −9 0). The (3 1, −2 1) unit cell is also shown for the (*R*,*R*)-bitartrate phase showing the packing within the chain.

Thus, it can be seen that the rows of the three bisuccinate molecules that assemble to form long chains possess different adsorbate−adsorbate juxtapositions and distances compared to the bitartrate structure. So, by simply looking at the unit cell within each chain, it can be seen that the (*R*,*R*)-tartrate chain possesses a (3 1, −2 1) structure growing in the [-114] direction, Figure 8b while the succinate chain possesses a (2 2, −2 0) or (2 0, −2 2) structure growing in [-112] and [1-12] directions, respectively, Figure 8a. Therefore, these small differences in organization must arise directly from second-order alterations in through-space lateral interactions and/or through-metal lateral interactions when OH groups are present at the chiral centers. Here, it is possible that the intramolecular H-bonds between the OH groups at the chiral center and the bonding carboxylate groups affect the detail of the metal−molecule interaction by influencing the precise distortion of the adsorbate backbone and the bonding carboxylate groups.

Finally, we consider the relative stabilities of the bisuccinate and bitartrate phases. Temperature programmed desorption (TPD) data from the bitartrate and the bisuccinate adlayer show explosive desorptions at around 440 and 600 K, Figure 9. Inspection of the thermal evolution products shows that no desorption of the molecular ion is observed, indicating that the data are not monitoring desorption of the whole adsorbate but rather the products of surface decomposition of adsorbed molecules. In other words, reaction limited desorption processes are observed, suggesting that the molecule−metal interaction is so strong that intramolecular bonds break prior to metal−

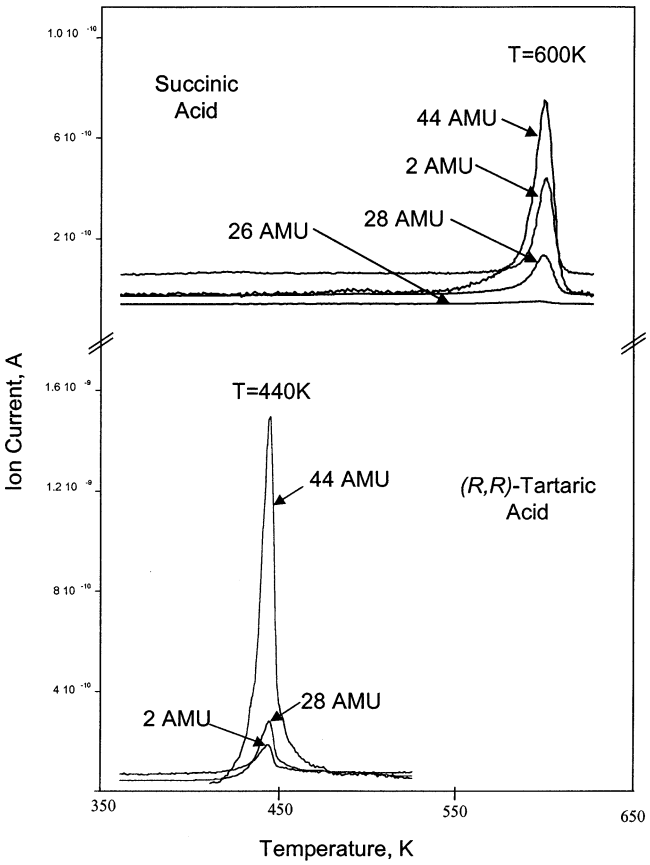

Figure 9. A comparison of the thermal stability of the bicarboxylate phases is demonstrated by TPD data for the (*R*,*R*)-bitartrate (1 2, −9 0) phase created on Cu(110) at 400 K and the bisuccinate phase, (9 0, −1 1) and (1 1, −9 0) structures created on Cu(110) at 400 K.

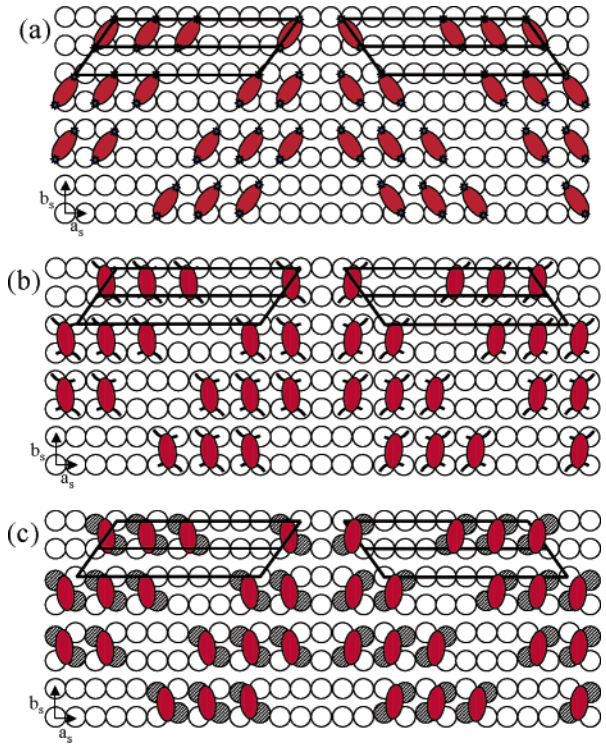

Figure 10. Three possible adsorption models for the bisuccinate/Cu(110) phase that would lead to (2 2, −9 0) and (9 0, −2 2) molecular packing but (1 1, −9 0) and (9 0, −1 1) LEED patterns. (a) Diagonal asymmetric adsorption of the bisuccinate molecule with the LEED scattering dominated by the bonding carboxylate groups (marked with *). (b) Molecularly distorted bisuccinate molecules with the LEED scattering repeat determined by the equivalent Cu−O sites (Cu−O_1 and Cu−O_4 or Cu−O_2 and Cu−O_3). (c) Local reconstruction of the Cu surface, where Cu atoms undergoing lateral displacement are depicted as gray circles, where the LEED scattering repeat is determined by the reconstructed Cu atoms.

molecule bonds, with the decomposition products, H_2, CO_2, and CO released in a sharp peak. From the TPD information, this process occurs some 150 K higher for the bisuccinate phase compared to the bitartrate, suggesting that the presence of the OH groups leads to a significant destabilization of the intramolecular bitartrate bonds. Although, the TPD data in this case give no information of the relative strengths of the molecule−metal interactions, it does point to very different temperature stabilities that arise in surface phases from small changes to the molecular structure.

(iii) Creation of Chirality in the Achiral Bisuccinate Phase. Of course, the most interesting aspect of the bisuccinate phase is that organizational chirality arises from the adsorption of an achiral molecule on an achiral surface. It is, therefore, interesting to analyze at which level chirality is introduced into the system. Here, the STM and LEED data give important clues. Whereas, the LEED data show the coexistence of two mirror (1 1, −9 0) and (9 0, −1 1) domains, the molecular positions imaged in the STM data possess molecular unit cells with a slightly different repeat structure, namely (2 2, −9 0) and (9 0, −2 2) structures, with a doubling of the repeat distance in the [-112] and [1-12] directions, respectively. We propose that such a result could arise from one of two possibilities. First, the LEED scattering could be dominated by the bonding carboxylate groups, with each molecule contributing two scattering centers. Whereas this halving of periodicity is most easily achieved by adsorbing the molecule diagonally across the close-packed rows as shown in Figure 10a, DFT calculations on this system[24] show that the molecule straddles straight across the close-packed rows with an attendant deformation of the molecular skeleton, as shown in Figure 10b. Such a deformation would naturally lead to inequivalence within each COO bonding unit, halving the LEED scattering repeat. Another possibility is that the LEED scattering is dominated not by the bonding carboxylate units but by reconstructions of the underlying metal. It is known that the succinate and tartrate structures possess significant surface interaction energies, calculated at 166 and 164 kJ mol^{-1}, respectively,[24] and are stable beyond 480 K at the surface, suggesting strong enough metal−molecule interactions that could trigger reconstructions. In addition, DFT calculations[24] show that adsorption of both molecules lead to a compressive strain along the [1-10] direction, with both preferring a Cu−Cu distance of 2.63 Å, which is greater than the bulk truncation close-packed Cu−Cu distance. We, therefore, propose that this strain could be relieved by lateral relaxations of the underlying Cu surface as, for example, depicted in Figure 10c, which would naturally lead to halving of periodicity in the required direction. For both options, we note that the halving of the periodicity along the [-112] and [1-12] directions require the deformation and/or reconstruction to be essentially chiral so that the two diagonal Cu−O_1 and Cu−O_4 units are equivalent and differ from the other two Cu−O_2 and Cu−O_3 units comprising the opposite diagonal. Chiral reconstructions and deformations of this type, which force the adsorbate to describe a chiral footprint at the surface, have been reported for the bitartrate/Ni(110) system.[5]

At present, the two structural models shown in Figure 10b,c cannot be differentiated on the basis of our data. However, what is most pertinent from the LEED data is that the halving of the molecular repeat distance *can only arise if asymmetry is introduced for the local adsorption unit*; i.e., the LEED data *directly point to the achiral bisuccinate adopting a local chiral adsorption motif*. Here, the creation of this chiral "synthon" is clearly adsorption-induced and must be intimately related to the nature of the metal−molecule bonding. Furthermore, it would seem from the general similarity of the trimer chain structure adopted that a similar influence must also be present when the bitartrate "synthon" is created; i.e. a doubled chiral influence may be present in this case: first, from the chiral centers of the molecule and, second, from the adsorption-induced asymmetry. This promises an interesting aspect of study for the future, both experimentally and theoretically.

(iv) Global and Local Chirality. From the adsorption models presented in Figure 8, it is evident that a similar manifestation of organizational surface chirality exists for the chiral bitartrate molecule and the achiral bisuccinate adsorbate. However, here the critical difference between the two systems also emerges: whereas for tartaric acid only one chiral handedness exists, which is sustained over the entire surface, for succinic acid both the chiral (9 0, −2 2) phase and its mirror image (2 2, −9 0) phase coexist at the surface, Figure 7a, so that by integrating over the entire surface one obtains an overall racemic conglomerate. This is a crucial difference in the expression of chirality between the two systems in that the bitartrate possesses global chirality while the bisuccinate is locally chiral but globally achiral.

A number of specifics may be envisaged that lead to this divergence of behavior. There are two major events that may propagate organized chiral domains at the surface: one, which leads to induction of point chirality, and the other, which leads to the induction of organizational chirality. From the data presented here it follows that, for our systems, the nature of the point chirality largely determines the organizational superstructure; i.e., the general nature of the bicarboxylate adsorption motif with its two COO−Cu bonding interactions is the "synthon" for the chiral organization of the bisuccinate and the bitartrate structures. Succinic acid possesses no inherent chirality, but our data show that a local chiral motif is created at the initial adsorption step, either due to molecular distortion and/or due to local chiral reconstruction. However, given the achirality of the adsorbing molecule, the nucleation of point chirality of one-handedness is energetically degenerate to creating point chirality of the opposite handedness so random adsorption processes will produce equal numbers of each, with asymmetric distortion/reconstruction manifesting in either of two mirror images, Figure 10c. Interestingly, our STM data show that growth direction is maintained from the nucleation point and random growth is not observed. Therefore, once nucleation has occurred, each local chiral adsorption unit thus created must generate a 2-fold chiral influence. First, it induces chirality in the supramolecular interactions; i.e., the placement of the next molecule is along a specific nonsymmetry direction and is energetically nondegenerate with respect to adsorption the same distance away in the reflection direction. Second, the point chirality of the unit must influence the point chirality of the adjacent adsorbing molecule, thus ensuring that the organization of the domain radiating from that nucleation point retains the same chirality. Our data on succinic acid indicate that these chiral supramolecular interactions are through-metal and/or through-space and do not involve direct hydrogen-bonding effects. Overall, nucleation points of both handedness exist equally so domains of either chirality will be propagated and coexist at the surface; i.e., the succinate system can only maintain chirality at the local level but is globally a racemic conglomerate.

For the (*R*,*R*)-bitartrate system, the major factors governing the creation of the chiral superstructure must be very similar to that for succinic acid; i.e., a similar molecular distortion and/or reconstruction must be induced by the bicarboxylate-Cu interaction, to create a similar superstructure. However, (*R*,*R*)-bitartrate yields a single domain of one-handedness only suggesting that the presence of the OH groups at the chiral centers crucially restricts the distortion/reconstruction to one-handedness only. We note that DFT calculations on (*R*,*R*)-bitartarte on Ni(110)[5] show an energy difference of 6 kJ mol^{-1} between the two mirror image distorted/reconstructed adsorption motifs, sufficient to ensure that over 90% of the nucleation points at 300 K would be of the lower energy form. The role of the OH groups as "chiral directors" of the supramolecular assembly is illustrated when adsorption of the (*S*,*S*)-bitartrate unit is examined, Figure 8b. Here, the rigid adsorption structure of the bitartarte unit forces the OH groups to lie in a uniquely defined direction that is reflected in space compared to the (*R*,*R*)-bitartrate unit. As a result, the energy preference of the local adsorption unit is switched to the opposite distortion/reconstruction, and thus, chiral lateral interactions are switched in direction and the induction and propagation of the chiral assembly occurs in the mirror image construct, leading to a mirror chiral surface. Therefore, from this work, one may conclude that overall global or local chirality is determined principally at the nucleation stage.

Finally, our work on the succinate system suggests that when the chiral centers are destroyed by replacing the OH groups with H, chirality at the local level may still exist in the system, but within a globally racemic system. This puts a different perspective on chiral enantioselective strategies for heterogeneous systems, where successful routes may not be restricted to designing a chiral modifier, but now also include the possibility of spontaneous chiral creation with simpler achiral modifiers where, subsequently, domains of the unrequired handedness can be neutralized by coadsorbing specific blocking molecules, as is often used in homogeneous enantioselective catalysis.

4. Conclusions

A detailed comparison of the molecular nature and two-dimensional order adopted by tartaric acid and succinic acid molecules on a Cu(110) surface is presented with close focus on how these aspects are altered by the fact that the former possesses two OH groups at the chiral centers, while the latter molecule only possesses H groups with consequent loss of chirality. A number of conclusions can be drawn from this body of work. First, the presence of the OH groups does not significantly affect the thermodynamically preferred chemical forms that are adopted, namely the doubly deprotonated bicarboxylate at low coverages ($\theta \leq {}^1/_6$ ML) and the singly

deprotonated monocarboxylate at higher coverages. However, the kinetics of forming the energetically preferred phases are significantly affected by the presence of the OH groups. In addition, the temperature stability of the bicarboxylate phases is significantly different. It can, therefore, be surmised that the conditions required for the creation and maintenance of a pertinent surface phase may alter substantially with small changes of molecular structure.

With respect to molecular self-assembly, a number of observations have been made. First, the primary force in determining the nature of the superstructures formed is the general chemical nature of the adsorbate and its metal−molecule interaction. Thus, for the monocarboxylate phase, the achiral c(4 × 2) assembly is adopted by both molecules. For the bicarboxylate phase, both the bisuccinate and the bitartrate show a similar trimer chain structure, which adopts a nonsymmetry growth direction that destroys the mirror planes associated with the Cu(110) surface; i.e., both give rise to two-dimensional organizational chirality. Overall, this general similarity points to the dominance of molecule−metal bonding in dictating packing, coverage, and the overall type of superstructures adopted. The effect of the OH groups at the chiral centers on the self-assembled structure is a second-order effect that leads to alterations in the detail of the assembly: the bitartrate phase creates a local (3 1, −2 1) chain structure growing in the [-114] direction, while the bisuccinate creates local (2 2, −2 0) and (2 0, −2 2) chain structures growing in the [-112] and [1-12] directions, respectively.

Finally, STM and LEED data show that the creation of chirality from the achiral succinate arises from adsorption-induced asymmetrization via molecular distortion and/or local reconstruction that creates point chirality. This chiral adsorption unit then acts as a "synthon" that generates the chiral organization via chiral lateral through-space and/or through-metal interactions. Since the succinate is inherently achiral, nucleation points of either chirality are generated with equal probability, so overall a racemic conglomerate is created. For the (*R*,*R*)-bitartrate system, the OH groups force the molecular distortion/reconstruction to adopt a favored chirality, which then generates one favored chiral domain only, bestowing the system with global chirality at the macroscopic scale. For the (*S*,*S*)-enantiomer, the OH group alignment is reflectionally flipped, and the mirror distortion/reconstruction is created, generating the mirror chiral organization. The OH groups are, therefore, important as chiral propagators or directors and enable asymmetry to be promoted to chirality. We point out that the mechanisms that induce chiral symmetry breaking in achiral systems remain little understood at present, and the succinic acid system provides a fascinating insight into aspects of this phenomenon. However, the creation of global chirality demands the more stringent condition that adsorption events and lateral interactions of one asymmetry are preferred over those with the reflectional asymmetry. For an achiral molecule on an achiral surface, this energy degeneracy cannot be lifted at all points of the adsorption process and, overall, a racemic surface is created. In that respect, the tartaric and succinic acid examples discussed here make a neat comparison between asymmetric versus chiral interactions.

Acknowledgment. We are grateful to the EPSRC for equipment grants and a Ph.D. studentship for V.H. and the Leverhulme Center for Innovative Catalysis for a Ph.D. studentship for M.O.L. We would also like to thank Dr. S. Barrett for many useful discussions on the LEED structures.

JA0382056